*Proc. Natl. Acad. Sci. USA*
Vol. 93, pp. 12287–12291, October 1996
Biophysics

# Patterning of functional antibodies and other proteins by photolithography of silane monolayers

(self-assembled monolayers/biotin/streptavidin/adsorption isotherms)

J. F. MOONEY*, A. J. HUNT†, J. R. MCINTOSH†, C. A. LIBERKO‡, D. M. WALBA‡, AND C. T. ROGERS*§

*Department of Physics, University of Colorado, Boulder, CO 80309-0390; †Department of Molecular, Cellular, and Developmental Biology, University of Colorado, Boulder, CO 80309-0347; and ‡Department of Chemistry and Biochemistry, University of Colorado, Boulder, CO 80309-0215

*Communicated by David M. Prescott, University of Colorado, Boulder, CO, August 15, 1996 (received for review February 9, 1996)*

ABSTRACT **We have demonstrated the assembly of two-dimensional patterns of functional antibodies on a surface. In particular, we have selectively adsorbed micrometer-scale regions of biotinylated immunoglobulin that exhibit specific antigen binding after adsorption. The advantage of this technique is its potential adaptability to adsorbing arbitrary proteins in tightly packed monolayers while retaining functionality. The procedure begins with the formation of a self-assembled monolayer of *n*-octadecyltrimethoxysilane (OTMS) on a silicon dioxide surface. This monolayer can then be selectively removed by UV photolithography. Under appropriate solution conditions, the OTMS regions will adsorb a monolayer of bovine serum albumin (BSA), while the silicon dioxide regions where the OTMS has been removed by UV light will adsorb less than 2% of a monolayer, thus creating high contrast patterned adsorption of BSA. The attachment of the molecule biotin to the BSA allows the pattern to be replicated in a layer of streptavidin, which bonds to the biotinylated BSA and in turn will bond an additional layer of an arbitrary biotinylated protein. In our test case, functionality of the biotinylated goat antibodies raised against mouse immunoglobulin was demonstrated by the specific binding of fluorescently labeled mouse IgG.**

We are interested in the development and application of techniques for protein patterning, especially for *in vitro* studies of protein function and for applications outside of the biological context (e.g., for artificial biomineralization and in biochemical sensors). In this paper we describe a general technique for producing two-dimensional patterns of functional protein on silicon dioxide surfaces by using a combination of self-assembled monolayers (SAMs) of alkyl silanes, albumin-alkyl adsorption, and biotin–avidin interactions. We illustrate the technique by generating two-dimensional patterns of functional goat antibodies raised against mouse immunoglobulins (GAM).

Our procedure begins with the formation of an *n*-octadecyltrimethoxysilane (OTMS)¶ SAM on a $SiO_2$ substrate. SAMs are increasingly important tools in the micro- and nanolithographic patterning of organic and inorganic materials. They have recently been used for selected area polypeptide synthesis (1), as barriers to chemical etching (2, 3), for the formation of microcrystals (4, 5) or microelectrodes (4), for creation of electrically conducting polypyrrole circuitry (6), for patterned water condensation (4), and for adhesion of cells (7–10) and proteins (8, 11–17). OTMS is one of the most widely used of the alkyl silanes for producing hydrophobic SAMs on $SiO_2$. The SAM can be selectively removed from the surface by ultraviolet (UV) exposure through a lithographic mask. The difference in adsorption of bovine serum albumin (BSA) to the exposed and unexposed regions of the surface creates a two-dimensional pattern of BSA with a surface coverage ≈50 times greater on the OTMS than on the exposed $SiO_2$. If the BSA is tagged with biotin, the pattern can be transferred to a second layer consisting of streptavidin, which bonds strongly and noncovalently to the biotin, but which does not adhere to exposed substrate. This streptavidin surface, in turn, provides for chemisorption of a third layer consisting, in principle, of any biotinylated molecule.

The SAMs were prepared as follows: We preclean our substrates, before SAM deposition, by sonication for 15 min in chromic/sulfuric acid glass cleaning solution (sulfuric acid/chromium trioxide/water, Fisher catalog no. SC88-1) and repeated rinsing in 18-MΩ·cm deionized water. The substrates were then dried with a blast of filtered $N_2$ gas to remove the bulk water. It is also critical that the glassware be dried in this way before the deposition to prevent undesirable polymerization of the OTMS. Covalent attachment of the silane groups was achieved by a 60-min sonication of the substrate in a solution of 5% (vol/vol) fresh OTMS in toluene with 0.5% *n*-butylamine as a catalyst. This is followed by a 30-min soak in the same solution. SAM quality was routinely checked with water contact angle measurements. When this measurement showed any degradation, new samples were prepared with fresh OTMS solution. Rinsing after removal from solution is not needed, since the substrate will spontaneously dewet. The temperature was kept below 23°C (18, 19). OTMS is deposited on a hydrophilic silicon dioxide substrate such that the long alkyl tails form a tightly packed monolayer while the Si attaches to the substrate through Si—O covalent bonds (18, 19). OTMS deposition leaves a hydrophobic surface which is chemically robust.

The OTMS can then be selectively removed by exposure to deep UV light (7, 20, 21) or by electron beam lithography (3, 22) to reveal the underlying hydrophilic $SiO_2$ surface. Thus OTMS offers a way to produce hydrophobic/hydrophilic patterns on $SiO_2$. The absence of the monolayer after exposure can be verified by atomic force microscopy [AFM (3), including lateral force microscopy (2, 6, 23)], scanning electron microscopy (4, 9, 11), x-ray photoelectron spectroscopy (7, 12, 13, 20), Fourier transform infrared spectroscopy (21), and water drop contact angles (7, 13).

For UV removal of OTMS, the efficiency of 250-nm light is 1/10 to 1/100 that of 193-nm light (7, 13, 20, 21). In this work, UV exposure was performed with a 1000-W Hg(Xe) arc lamp run at 440 W and delivering 1.05 W/cm$^2$ of broad-band radiation. Only 10 mW/cm$^2$, at a distance of 25 cm from the

The publication costs of this article were defrayed in part by page charge payment. This article must therefore be hereby marked "*advertisement*" in accordance with 18 U.S.C. §1734 solely to indicate this fact.

Abbreviations: SAM, self-assembled monolayer; OTMS, *n*-octadecyltrimethoxysilane; GAM, goat antibodies raised against mouse immunoglobulin; DAG, donkey antibodies raised against goat immunoglobulin; FITC, fluorescein isothiocyanate; AFM, atomic force microscopy; BET, Brunauer–Emmett–Teller.

§To whom reprint requests should be addressed.

¶Note that *n*-octadecyltrichlorosilane (OTCS) is frequently cited in the literature as a compound for the formation of SAMs and is more reactive than OTMS.

collimating lens, comes from the 243.7-nm Hg emission peak. There are also peaks at 194 nm and 185 nm, but they are attenuated to <0.5 mW/cm$^2$ due to the optics and arc lamp's quartz envelope. Exposure of the OTMS monolayer through a Ni grid, for 10 min on a polished $SiO_2$-on-Si substrate or 16 min on a pure glass substrate, was sufficient for AFM images to show clear square depressions roughly 2 nm deep (close to the length of the alkyl tail); these differences in exposure times probably arise from the greater reflectivity of the Si substrate. These AFM images convey topographical information, but they do not reveal the full chemical status of the surfaces (in lateral force mode, some chemical surface characterization can be achieved) (2, 6, 23). Despite the appearance of patterns in AFM scans, greater UV doses were required to alter the BSA adsorption to OTMS. When exposing the sample with a chromium-coated quartz mask, longer exposure times are required to remove the OTMS. A ¼-inch (6.4-mm)-thick quartz attenuator was also added in the beam path to reduce heating of the mask and substrate, which may damage the OTMS layer in contact with the chromium. The addition of the mask and attenuator requires an exposure of 100 min due to attenuation of the UV.

BSA is a blood protein that typically binds the hydrophobic tails of 1 to 3 mol of fatty acids per mol of BSA (24). The adsorption of BSA on a surface depends on the nature of the substrate. At solution concentrations below 0.05 mg/ml BSA will adsorb to a hydrophobic surface (methylated silica) at virtually any pH, while it binds to hydrophilic glass in only a narrow range around pH 5.5 (25). It therefore seemed likely that at any pH sufficiently removed from 5.5, BSA would adsorb more strongly to OTMS (with its long alkyl chain acting like a nonpolar fatty acid) than to $SiO_2$.

To verify this differential adsorption behavior we measured adsorption isotherms for fluorescein isothiocyanate (FITC)-tagged BSA (Sigma catalog no. A9771) on OTMS and on the bare $SiO_2$ substrates. Fig. 1 shows these data as well as some of the adsorption isotherms of the OTMS after UV exposure. The curves shown are fits to the Brunauer–Emmett–Teller (BET) isotherm (26, 27):

$$\frac{x}{x_m} = \frac{1}{1-(c/c_s)} - \frac{1}{1+(\tau-1)(c/c_s)}, \qquad [1]$$

where $x$ and $c$ are the surface and solution concentrations, respectively, of BSA, $x_m$ is the surface coverage of a monolayer of BSA, and $c_s$ is the saturation concentration of BSA in the buffer, measured to be 370 ± 20 mg/ml (5.4 mM). $\tau$ is a dimensionless fitted parameter of the curve and roughly represents the ratio of the characteristic time a BSA molecule spends adhered to the tested surface compared with the time it would spend adhered to a pure solid BSA surface under identical solution conditions (27). The BET isotherm fits serve as qualitative guides for understanding the adsorption behavior.

To study the BSA adsorption we have employed a flow cell made by fixing the sample to a glass slide with silicon vacuum grease [Dow Corning high vacuum grease (silicon-based lubricant)], with ≈75-μm-thick coverslip fragments used as spacers. The cell allows a series of solutions to flow across the sample while minimizing its exposure to air, which would increase the rate of fluorescence bleaching and the probability of protein denaturation. First the solution of FITC-BSA, dissolved in BRB-80 buffer (80 mM Pipes/1 mM $MgCl_2$/1 mM EGTA adjusted to pH 6.9 with 1 M KOH), was made to flow into the cell and allowed contact with the sample for 10 min. We then flushed the cell with 6 cell volumes of the BRB-80 buffer to remove unattached protein.

The amount of adsorbed protein was measured by quantifying the fluorescence that remained bound to the glass 1 min after buffer flow. A conversion from fluorescence intensity to concentration of protein was obtained by measuring the intensity of known solution concentrations of fluorescently labeled protein in a volume defined by the image plane area and the cell depth. The values of surface concentration were calculated as follows: The intensity of the sample is measured by fluorescence microscopy with a CCD (charge-coupled

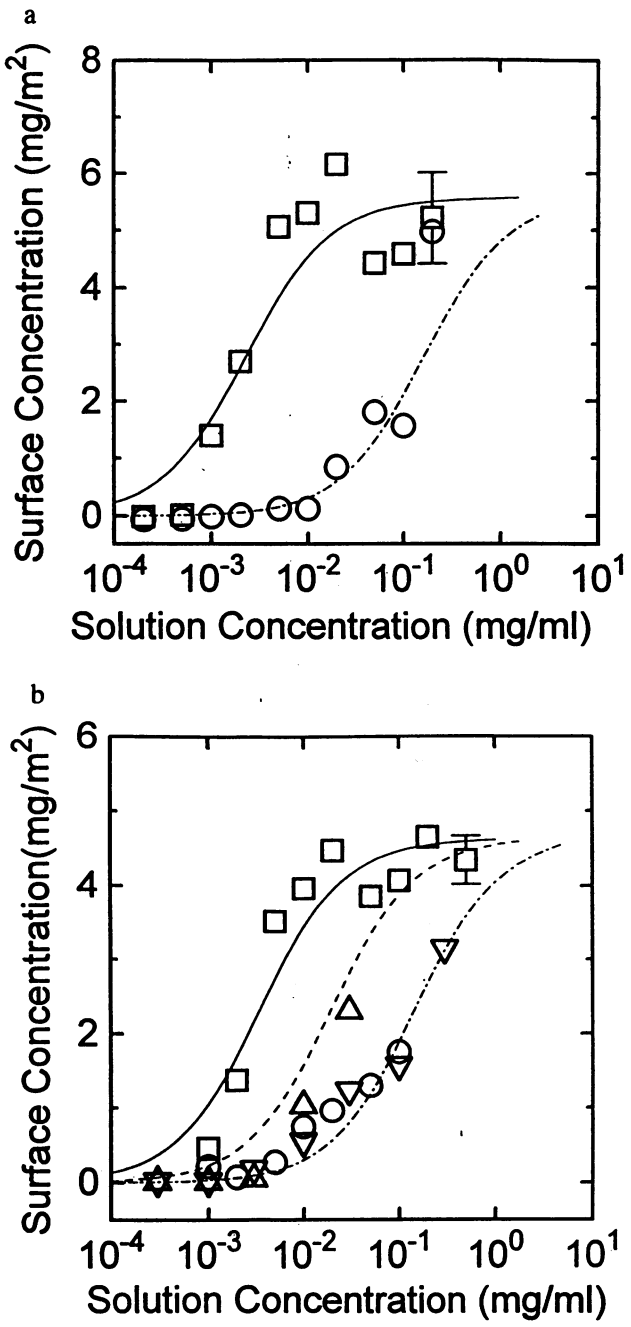


FIG. 1. Adsorption isotherms for FITC-labeled BSA measured by fluorescence intensities. (*a*) Glass substrate: □ indicates adsorption on OTMS-coated glass; ○, on bare glass. Solid and dash-dot curves are fits to BET isotherms as described in text. Parameters are $c_m$ = 370 mg/ml, $x_m$ = 5.56 mg/m$^2$, $\tau = 1.6 \times 10^5$ on OTMS, and $\tau = 2.3 \times 10^3$ on glass. (*b*) Oxidized silicon substrate: □ indicates adsorption on OTMS-coated thermally oxidized Si crystal; ○, on bare thermally oxidized Si crystal; △, OTMS after 60-min UV exposure; ▽, OTMS after 85-min UV exposure. Solid, dash, and dash-dot curves are fits to BET isotherms for the unexposed OTMS, 60-min UV exposure, and 85-min UV exposure. The parameters are $c_m$ = 370 mg/ml and $x_m$ = 4.63 mg/m$^2$ on all three fits, with $\tau = 1.1 \times 10^5$, $\tau = 1.9 \times 10^4$, and $\tau = 2.6 \times 10^3$ for the unexposed, 60-min exposure, and 85-min exposure, respectively.

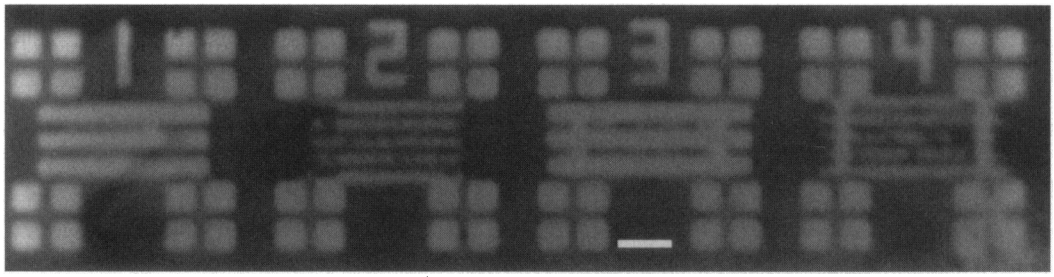


FIG. 2. Fluorescence micrograph taken with a CCD camera of FITC-BSA adsorbed on a patterned OTMS surface on a silicon wafer. The inset marker bar is 10 $\mu$m wide, and the smallest lines of the pattern are 1 $\mu$m wide.

device) camera. The image is then exported to a computer to analyze the regional statistics of intensity. The number of molecules is calculated, using the solution calibration above. The accuracy of this technique is good to a factor of 2, due to the calibration of intensity from the protein solution; the relative precision is estimated at 8%.

Preliminary results indicated that BSA adsorption onto OTMS is an exponential function of time with a characteristic time constant of $\approx$3 min at 0.01 mg/ml solution of BSA on OTMS, and <10 sec at 0.1 mg/ml. There was, however, no substantial desorption of BSA after 1 hr of exposure to protein-free buffer. The adsorption differential between the OTMS and the substrate allows the chemical nature of the UV-exposed regions to be compared with those shielded by the mask. Although OTMS is topographically removed by a 10- to 16-min exposure, Fig. 1*b* shows that 85 min of exposure to UV is required before the surface adsorbs BSA at a level comparable to that of the original substrate. Above 0.01 mg/ml BSA, adsorption on OTMS-coated glass levels out at 5.6 $\pm$ 1.7 mg/m$^2$, and it maintains this level at least to 0.5 mg/ml. On thermally oxidized silicon, coated with OTMS, the adsorption plateau was measured at 4.6 $\pm$ 0.2 mg/m$^2$, the same as on a glass substrate within experimental error. Fair and Jamieson calculate (28) that a close-packed monolayer of BSA should have a surface concentration of 2.5 mg/m$^2$, assuming BSA (molecular mass = 69 kDa) to be an ellipsoid with major and minor axes of 14.0 nm and 3.8 nm and that it adsorbs with its major axis parallel to the surface. Our measured surface concentrations are somewhat above this value. However, given inherent systematic uncertainties in converting fluorescent yield to surface concentration and our observed plateau in adsorption, we interpret our results as indicating that BSA forms a monolayer on OTMS. According to a BET model, as the solution concentration increases, the surface adsorption will at some point rise beyond the monolayer level. However, our attempts to measure this multiple layer adsorption regime for BSA have been frustrated by the rapid desorption of subsequent layers when BRB-80 is made to flow in to remove the unabsorbed BSA.

The adsorption results shown in Fig. 1 indicate a significant adsorption differential between OTMS and $SiO_2$ surfaces. They imply that *patterned* OTMS would be effective at producing high-definition monolayer patterns of BSA. From Fig. 1 it is evident that the largest adsorption differential available in BRB-80 is 24:1. We have investigated the influence of pH on adsorption: By replacing Pipes buffer with Hepes, the pH can be extended from 6.9 to 8.2, where the differential increases to 50:1 with BSA at 4 $\mu$g/ml (Pipes and Hepes are standard biological buffers obtained from Sigma, catalog nos. P6757 and H3375, respectively).

Fig. 2 shows a fluorescence micrograph of such a pattern of FITC-labeled BSA. In this case, the OTMS surface was prepared on a commercially available Si wafer, thermally oxidized to produce a 200-nm-thick surface layer of $SiO_2$ (2-inch P<100> wafers, Silica Source Technology, Tempe, AZ). The patterned OTMS shows the preferential adsorption of the BSA to the OTMS regions. The fluorescently labeled BSA was made to flow across the substrate in a cell as described above, and the cell was rinsed with protein-free buffer. Fluorescence microscopy was used to image the resulting patterns. This process reproducibly results in monolayer BSA adsorption, patterned with resolution limited only by the resolution of the UV lithography.

These BSA patterns are easily extended to additional proteins through the use of biotin and streptavidin. Biotin is a small molecule (244 Da) that can be attached to most proteins through a succinimide ester (29). Streptavidin is a globular protein (60,000 Da) with four binding sites for biotin on two opposing sides (30). In our process, biotinylated BSA at 4 $\mu$g/ml is made to flow across the surface to create a biotin pattern. After 10 min, we pass 6 cell volumes of buffer solution and then 6 cell volumes of streptavidin, 18 $\mu$g/ml, tagged with FITC, through the cell. The streptavidin is allowed 2 min of adsorption before it is rinsed away with another 6 cell volumes of buffer. Fig. 3*a* shows a fluorescence micrograph of the streptavidin chemisorbed in a pattern from the same mask as the fluorescent BSA of Fig. 2. Our measurements suggest that 2.8 $\pm$ 0.5 molecules of streptavidin chemisorb to each molecule of BSA. We have determined that streptavidin alone does not exhibit monolayer scale adsorption to either the OTMS or the bare substrate, thus necessitating the biotinylated BSA as an intermediate.

The biotinylation[‖] of crystallized and lyophilized BSA (97–99% pure bovine albumin, Sigma catalog no. A4378) has some impact on its adsorption to the surfaces used here. Increasing levels of biotinylation of the BSA increases the adsorption of the BSA to untreated $SiO_2$. In BRB-80 buffer, BSA biotinylated at 8–12 molecules of biotin per molecule of BSA actually has a higher affinity for glass than for OTMS. However, when the Pipes was replaced with Hepes and the pH was adjusted to 7.49, BSA biotinylated with 140 $\mu$g of biotin ester per 1 mg of BSA followed by FITC-labeled streptavidin, in the same buffer, emitted a fluorescence signal greater on the OTMS than on the $SiO_2$ regions by a factor of $\approx$32. We also found that added salts decrease adsorption on both the OTMS and glass. Optimization of all these factors may eventually lead to even higher adsorption differentials.

The streptavidin pattern provides a surface of general utility for chemisorbing other biotinylated proteins. As an example, we have used these streptavidin patterns to bind biotinylated antibodies and verify selective adsorption of the target antigen by two-color fluorescence microscopy. Fig. 3 *Left* shows a collection of streptavidin patterns imaged with a fluorescein filter set. These patterns were used to adhere a layer of biotinylated goat IgG antibodies raised against mouse immu-

[‖]Biotinylation method from BioSearch, San Rafael, CA: Biotinamidocaproate *n*-hydroxysuccinimide ester is prepared at 1 mg/ml in dimethyl sulfoxide and added at various volumes to 1 ml of 1 mg/ml BSA. This solution is allowed to react at room temperature for 4 hr. The solution is then dialyzed four times in 2 liters of phosphate buffer (20 mM $Na_2HPO_4$/150 mM NaCl, pH to 7.4 with 1 M HCl).

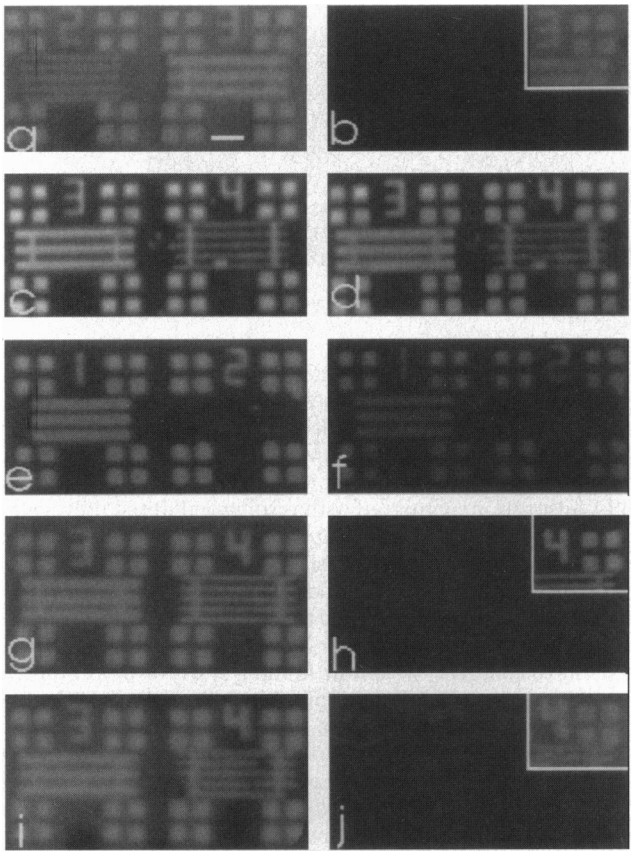


FIG. 3. Fluorescence micrographs of proteins adsorbed on a patterned OTMS surface. Images were taken through a fluorescein filter set (*Left*) or through a rhodamine filter set (*Right*). (*a*) Image of a patterned streptavidin layer tagged with FITC. The layer is visible, attached to the underlying biotinylated BSA. The inset marker bar is 10 $\mu$m wide. (*b*) Filters set up for rhodamine fluorescence to show minimal crossover from the fluorescein. The upper-right corner has had the intensity increased by 16× to show the weak signal. (*c*) A new substrate with a streptavidin image in the fluorescein spectrum after exposure to rhodamine-labeled mouse antibodies. (*d*) The same location, using the rhodamine filter set to reveal the mouse immunoglobulin layer bound to the pattern through the biotinylated goat antibodies raised to mouse immunoglobulin (GAM), which are attached to the streptavidin layer. *e*, *g*, and *i* are the streptavidin images that are associated with *f*, *h*, and *j* in the rhodamine wavelengths after exposure to rhodamine-labeled rat, goat, and donkey antibodies, respectively. In the upper right corner of *b*, *h*, and *j* the signal has been increased by 16× to be visible to the eye. The images show the relative brightness of the crossover of the fluorescein into the rhodamine spectrum as well as the low levels of adhesion of the goat and rabbit antibodies. Taken together, these images show that the surface-bound GAM remains functional in selective binding of the target mouse antibodies.

noglobulin (GAM; Jackson ImmunoResearch catalog no. 115–065-003). In Fig. 3 *Right* we show images taken with a filter set appropriate for rhodamine-tagged protein. These images show adsorption detected for a variety of proteins. Fig. 3*b* shows the rhodamine image before the target protein and demonstrates that the crossover of the fluorescein into the rhodamine spectrum is minimal. Fig. 3*d* shows local area binding of tetramethylrhodamine-labeled mouse immunoglobulin (Jackson ImmunoResearch catalog no. 209-025-082) to the biotinylated GAM which were adhered to the fluorescein-labeled streptavidin pattern in Fig. 3*c*. Here, after the patterning of streptavidin, 6 cell volumes of 2 $\mu$g/ml biotinylated GAM were passed into the cell for 2 min, during which time the goat antibodies chemisorb to the streptavidin layer. Adsorption is followed by a buffer rinse to remove unbound protein. To test functionality of the bound GAM, 6 cell volumes of mouse IgG immunoglobulins tagged with a tetramethylrhodamine fluorescent marker were passed into the cell and allowed 2 min for binding to the adsorbed GAM. After 6 cell volumes of buffer, fluorescence of the sample revealed the pattern in Fig. 3*d*. Thus, the biotinylated and chemisorbed GAM is still functional at recognizing and binding mouse antibodies. As a control, FITC-BSA and tetramethylrhodamine-tagged rat, goat, and rabbit immunoglobulins were made to flow across the GAM surface in place of the mouse immunoglobulins. The adsorption of the rat immunoglobulin was only 18% of the adsorption of the mouse IgG, while the adsorption of the goat and rabbit IgG was at low enough levels that it was difficult to quanitatively separate the IgG signal from the FITC crossover within the uncertainty of 3% of the mouse antibody rhodamine signal level. Various images in the fluorescein wavelengths of the FITC-labeled streptavidin patterns are shown in Fig. 3 *e*, *g*, *i*, and *k*. The corresponding images in the rhodamine wavelengths after exposure to mouse, rat, donkey, and rabbit IgG antibodies are presented in Fig. 3 *d*, *f*, *h*, and *j*, respectively. These images demonstrate that the GAM surface retains its functionality for selective adsorption of the target mouse immunoglobulin.

To estimate the fraction of the biotinylated and adsorbed GAM molecules that remained functional, we studied the goat antibody surface as follows: Subsequent to streptavidin patterning of GAM, rhodamine-labeled donkey IgG antibodies raised against goat immunoglobulin (DAG; Jackson ImmunoResearch catalog no. 705-025-003), at 2 $\mu$g/ml, were made to flow across the surface to determine whether the GAM was chemisorbed in a form recognizable to the DAG. The same pattern visible in the streptavidin fluorescence was then also visible with rhodamine filters, indicating that the surface is recognizable as goat antibody. The level of DAG binding calculated from fluorescent signals was 0.51 mg/m$^2$, indicating 1 DAG molecule per 37 streptavidin molecules adsorbed on the surface (using a DAG mass of 150 kDa from Jackson ImmunoResearch). Thus, the GAM layer is still largely recognized as goat immunoglobulin by the DAG and the density of the GAM is on the order of a monolayer coverage. In contrast, the fluorescence measurements with rhodamine-labeled mouse IgG (instead of the DAG), such as Fig. 3*d*, revealed that the mouse immunoglobulin was bound at a concentration of 0.22 mg/m$^2$. Using a mass of 160 kDa from Jackson ImmunoResearch, this implies 1 mouse immunoglobulin molecule per 83 streptavidin molecules on the surface. If we assume that steric hindrance allowed only 1 DAG antibody to bind to each GAM on the surface, then these results indicate that the density of the GAM is also at 1 GAM per 37 streptavidins and that 45% of the GAM monolayer retains its ability to bind a mouse immunoglobulin. If 2 DAG molecules on average bind to each GAM molecule, then the density of the GAM is 1 GAM per 74 streptavidins, and the functionality of the GAM would be estimated at ≈90%. Effects of fluorescent bleaching were minimized by measuring the fluorescence after less than 30 sec of exposure under the microscope. We are presently attempting a more direct measurement of the percent functionality through the use of biotinylated and fluorescently tagged GAM. However, our present results show that the surface remains largely functional.

In this paper we have described a method to adhere functional antibodies to a patterned surface. Patterned OTMS on $SiO_2$ provides a selective surface on which to adsorb a monolayer of streptavidin via a biotinylated BSA intermediate. The streptavidin layer can then be used to attach a variety of biotinylated proteins. Our results suggest at least two distinct ways to generalize the process for patterned adhesion of arbitrary functional proteins. First, our demonstration of antibody function suggests that any protein for which an antibody is available can be localized to the pattern by means of antibody binding. Second, given the variety of proteins that

have been demonstrated to retain function after biotinylation, one can imagine direct replacement of biotinylated antibody with arbitrary biotinylated protein. The wide availability of antibodies and biotinylated proteins suggests that our procedure is generally applicable for *in vitro* protein studies and the technological utilization of protein function.

We acknowledge support of this project by the Office of Naval Research through Grant N00014-94-1-0621.

1. Fodor, S. P. A., Read, J. L., Pirrung, M. C., Stryer, L., Lu, A. T. & Solas, D. (1991) *Science* **251,** 767–773.
2. Sugimura, H., Nakagiri, N. & Ichinose, N. (1995) *Appl. Phys. Lett.* **66,** 3686–3688.
3. Lercel, M. J., Tiberio, R. C., Chapman, P. F., Craighead, H. G., Sheen, C. W., Parikh, A. N. & Allara, D. L. (1993) *J. Vac. Sci. Technol. B* **11,** 2823–2828.
4. Kumar, A., Biebuyck, H. A. & Whitesides, G. M. (1994) *Langmuir* **10,** 1498–1511.
5. Ogawa, S. Fan, F.-R. F. & Bard, A. J. (1995) *J. Phys. Chem.* **99,** 11182–11189.
6. Gorman, C. B., Biebuyck, H. A. & Whitesides, G. M. (1995) *Chem. Mater.* **7,** 526–529.
7. Hickman, J. J., Bhatia, S. K., Quong, J. N., Shoen, P., Stenger, D. A., Pike, C. J. & Cotman, C. W. (1994) *J. Vac. Sci. Technol. A* **12,** 607–616.
8. Margel, S., Vogler, E. A., Firment, L., Watt, T., Haynie, S. & Sogah, D. Y. (1993) *J. Biomed. Mater. Res.* **27,** 1463–1476.
9. Singhvi, R., Kumar, A., Lopez, G. P., Stephanopoulos, G. N., Wang, D. I. C., Whitesides, G. M. & Ingber, D. E. (1994) *Science* **264,** 696–698.
10. Stenger, D. A., Georger, J. H., Dulcey, C. S., Hickman, J. J., Rudolph, A. S., Nielsen, T. B., McCort, S. M. & Calvert, J. M. (1992) *J. Am. Chem. Soc.* **114,** 8435–8442.
11. Lopez, G. P., Biebuyck, H. A., Härter, R., Kumar, A. & Whitesides, G. M. (1993) *J. Am. Chem. Soc.* **115,** 10774–10781.
12. Bhatia, S. K., Hickman, J. J. & Ligler, F. S. (1992) *J. Am. Chem. Soc.* **114,** 4432–4433.
13. Bhatia, S. K., Teixeira, J. L., Anderson, M., Shriver-Lake, L. C., Calvert, J. M., Georger, J. H., Hickman, J. J., Dulcey, C. S., Schoen, P. E. & Ligler, F. S. (1993) *Anal. Biochem.* **208,** 197–205.
14. Fragneto, G., Thomas, R. K., Rennie, A. R. & Penfold, J. (1995) *Science* **267,** 657–660.
15. Ichinose, N., Shimo, N. & Masuhara, H. (1995) *Chem. Lett.* **1995,** 237–238.
16. Amador, S. M., Pachence, J. M., Fischetti, R., McCauley, J. P., Jr., Smith, A. B., III, & Blasie, J. K. (1993) *Langmuir* **9,** 812–817.
17. Duan, C. & Meyerhoff, M. E. (1995) *Mikrochim. Acta* **117,** 195–206.
18. Parikh, A. N., Allara, D. L., Azouz, I. B. & Rondelez, F. (1994) *J. Phys. Chem* **98,** 7577–7590.
19. Brzoska, J. B., Azouz, I. B. & Rondelez, F. (1994) *Langmuir* **10,** 4367–4373.
20. Dulcey, C. S., Georger, J. H., Krauthamer, V., Stenger, D. A., Fare, T. L. & Calvert, J. M. (1991) *Science* **252,** 551–554.
21. Calvert, J. M., Georger, J. H., Peckerar, M. C., Pehrsson, P. E., Schnur, J. M. & Schoen, P. E. (1992) *Thin Solid Films* **210/211,** 359–363.
22. Tiberio, R. C., Craighead, H. G., Lercel, M., Lau, T., Sheen, C. W. & Allara, D. L. (1993) *Appl. Phys. Lett.* **62,** 476–478.
23. Wilbur, J. L., Biebuyck, H. A., MacDonald, J. C. & Whitesides, G. M. (1995) *Langmuir* **11,** 825–831.
24. Peter, T. & Reed, R. G. (1978) in *Transport by Protein*, FEBS Symposium 50, eds. Blauer, G. & Sund, H. (de Gruyter, Berlin), pp. 63–64.
25. MacRitchie, F. (1972) *J. Colloid Interface Sci.* **38,** 484–488.
26. Brunauer, S., Emmett, P. H., Teller, E. (1938) *J. Amer. Chem. Soc* **60,** 309–312.
27. Gregg, S. J. & Sing, K. S. W. (1967) *Adsorption, Surface Area and Porosity* (Academic, London), p. 45.
28. Fair, B. D. & Jamieson, A. M. (1980) *J. Coll. Inter. Science* **77,** 525.
29. Costello, S. M., Felix, R. T. & Giese, R. W. (1979) *Clin. Chem. (Washington, DC)* **25,** 1572–1580.
30. Chaiet, L. & Wolf, F. J. (1964) *Arch. Biochem. Biophys.* **106,** 1–5.